EUROPEAN FUSION DEVELOPMENT AGREEMENT

EFDA–JET–CP(03)03-11

P.U. Lamalle, F. Durodié, A. Whitehurst, R.H. Goulding, P.M. Ryan
and JET EFDA Contributors

# Three-Dimensional Electromagnetic Modelling of the JET ITER-Like ICRF Antenna

# Three-Dimensional Electromagnetic Modelling of the JET ITER-Like ICRF Antenna

P.U. Lamalle[1], F. Durodié[1], A. Whitehurst[2], R.H. Goulding[3], P.M. Ryan[3]
and JET EFDA Contributors*

*[1]Laboratory for Plasma Physics, Association EURATOM-Belgian State, TEC, Royal Military Academy, B-1000 Brussels, Belgium.*
*[2]EURATOM/UKAEA Fusion Association, Culham Science Centre, Abingdon, OX14 3DB, UK*
*[3]Oak Ridge National Laboratory, USA.*
** See annex of J. Pamela et al, "Overview of Recent JET Results and Future Perspectives", Fusion Energy 2000 (Proc. 18th Int. Conf. Sorrento, 2000), IAEA, Vienna (2001).*

Preprint of Paper to be submitted for publication in Proceedings of the
15th Topical Conference on Radio Frequency Power in Plasmas
(Moran, Wyoming, USA 19-21 May 2003)

**ABSTRACT.**
During its design phase, the JET ITER-Like ICRF antenna array has been modeled in great detail with the 3D electromagnetic software CST MICROWAVE STUDIO®. The resulting rf field and current density patterns have guided the optimization of the antenna feeder shapes, leading overall to a strong reduction (~25%) of the maximum electric field, and to a factor-of-three reduction of the inhomogeneity of rf current at the matching capacitors. The computed frequency response of the array is now used in matching studies and development of a control algorithm. Comparison with the experimental frequency response of the High Power antenna Prototype developed by ORNL and PPPL shows fair agreement.

## 1. INTRODUCTION

As of today, successful quantitative predictions of the coupling properties of ICRF antennae on plasma remain to be demonstrated. This requires an accurate computation of both active and reactive antenna properties. The reactance evaluation demands detailed calculation of near fields and self-consistent surface currents on complex metallic structures, and was probably the weakest point of earlier simulations. Accordingly, a key area of work during the design of the JET ITER-Like ICRF antenna [1] has been the selection, development and application of improved 3D electromagnetic simulation tools, which have become quite powerful and user-friendly since the last generation of antennae were designed. In the present paper, we summarize the results of simulations of the JET ITER-Like antenna array with the CST MICROWAVE STUDIO ® (MWS) software [2], which was used to optimize the complex 3D geometry of the antenna feeders. Operation of the antenna will provide a crucial assessment of this effort, to benefit future designs, the ITER one in particular. A first benchmark of vacuum code predictions against recent measurements on the High Power Prototype antenna developed by ORNL and PPPL [3] has successfully been carried out. A comprehensive 3D study of the current JET A2 antenna, to be reported elsewhere, has also been initiated and will allow detailed comparison with ICRF coupling data.

## 2. THE ANTENNA MODEL

Figure 1 shows the main features of the MWS RF antenna model, fully consistent with the drawing office blueprints: antenna box, coaxial feeds, tapered feeder sections through the back of the box, connected to oblique feeder sections by capacitor protection plates; radiating straps, Faraday shield, poloidal and toroidal septa. Note that the poloidal and toroidal curvatures of the system, the finite thickness of all conductors and the individual rods of the shield are taken into account. Reduced models of 1 or 2 straps allow investigating specific issues. MWS solves Maxwell's equations with the finite integration technique [4] and finite differencing in time.

Typical outputs are the array scattering parameters as a function of frequency, and 3D field maps at selected frequencies. The software allows various time-dispersive media such as magnetized ferrites, but does not include a magnetized plasma dielectric tensor. The curved solid shown in the

right view Figure 1 is a high permittivity dielectric mimicking plasma loading. Its steep edge is representative of worst-case coupling conditions to a high-power ELMy H mode discharge, and its dielectric constant is chosen to reproduce the magnetosonic wavelength at a typical frequency and toroidal wavenumber. The boundary conditions are a metal back plane (not shown) and radiation conditions on all other boundaries, which amounts to assuming single pass absorption in the plasma bulk and absence of global toroidal eigenmodes. There is clearly scope to improve this loading model for future comparisons with plasma heating experiments. Nevertheless, the design optimization has proceeded by evolution of an initial drawing, and comparison of the RF characteristics of the successive geometries has been performed in normalized conditions (unit currents at the strap short-circuits), which strongly reduces the influence of assumptions on resistive loading. The ad-hoc dielectric then mainly contributes through its influence on the antenna reactance.

## 3. OPTIMIZATION OF THE FEEDER REGION

The purpose of this activity was to improve the initial design and widen the operational domain of the launcher. This required compromise between several conflicting goals: (a) minimizing the maximum electric field, which requires maximum gaps between conductors and smooth transitions between feeder sections; (b) minimizing input voltages (at fixed radiating strap geometry), which requires the shortest feeders possible and small gaps for low inductance; (c) achieving voltage homogeneity between radiating loops for optimal operation close to limits; (d) achieving maximum azimuthal symmetry for the rf current density at the feeder-capacitor connections to make best use of capacitor specifications. The main constraints were mechanical strength, JET port size, vessel poloidal curvature, access for capacitor cooling through the feeders, requirement to shield the capacitors from direct heat flux, space requirements for RF gaskets at the back of the antenna box. The result of many progressive design modifications is summarized on Figures 2 and 3:

The initial design had tapered oblique feeder sections and racetrack-shaped horizontal sections directly connected to the capacitor sliding contact flange; the final layout has thinner septa, wider oblique sections, capacitor shielding plates, wide cylindrical sections through the antenna box connecting to the flange, and the capacitors moved outward by a few cm. Overall these improvements reduce the maximum electric field by ~25% (up to 40% at the capacitor flange). Moreover, Figure 3 shows a reduction of the surface current inhomogeneity at the flange by a factor of 3, which decreases peak and total dissipation on the capacitors.

## 4. FREQUENCY RESPONSE

The input scattering matrix of the loaded antenna array has been obtained (Fig.4) and is currently used in matching studies [5]. Maximum strap reactances are found smaller than the upper estimate initially used to define capacitor specifications. Final design refinements are under study to reduce poloidal cross-talk S23 between inner straps (Fig.5). Measurements on the antenna prototype [3] are well reproduced by its MWS model (Fig.6), which increases confidence in other predictions.

## CONCLUSIONS

The design of the JET ITER-Like antenna has triggered unprecedented RF modelling of ICRF antennae with the most advanced tools available today. This was instrumental to optimize the details of the strap and feeder geometry: since the early design, the maximum electric field has been reduced by ~25% (up to 40% near the capacitors), and the azimuthal inhomogeneity of currents near the capacitors has been reduced by a factor of three. The modelling is now used to adjust the final design of the equatorial septum, to reduce the cross-talk between straps, and to assess its influence on the matching performance using the computed input impedance matrix. Successfulcode benchmarking against measurements on the High Power Prototype of a quarter antenna increases confidence in the results. Based on this work, the use of the ITER-like antenna on JET will not only provide demonstration of ICRF coupling in ITER-relevant conditions, but also enable a validation of modelling useful to progress in the understanding of RF coupling in fusion devices, and useful to optimize the design of the ITER antenna itself.

## ACKNOWLEDGEMENTS

This work has been performed under the European Fusion Development Agreement. It has greatly benefited from numerous discussions within the JET ITER-Like antenna Design Team [1], with Dr R Ehmann and the CST GmbH Support Team. We gratefully thank Dr J Paméla for his stimulating support.

## REFERENCES

[1]. Durodié, F., et al., these Proceedings.

[2]. CST MICROWAVE STUDIO User Manual, Version 4.0, CST GmbH, Darmstadt, Germany, 2002; http://www.cst-world.com.

[3]. Goulding, R.H., et al., these Proceedings.

[4]. Weiland, T., International Journal of Numerical Modelling: Electronic Networks, Devices and Fields 9, New York: Wiley, 1996, pp.295-319.

[5]. Lamalle, P. U., et al., these Proceedings.

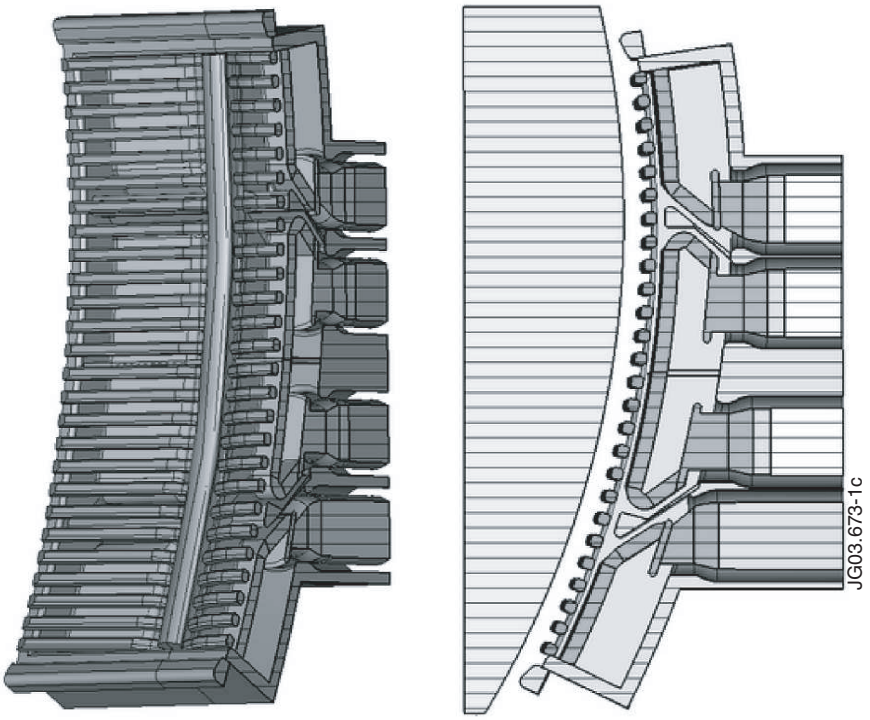


*Figure 1: RF MWS model of the ITER-Like antenna (final design layout). Left: partial front view; right: side view with dielectric loading (both are cut vertically through the axes of 4 matching capacitors to show feeder profiles).*

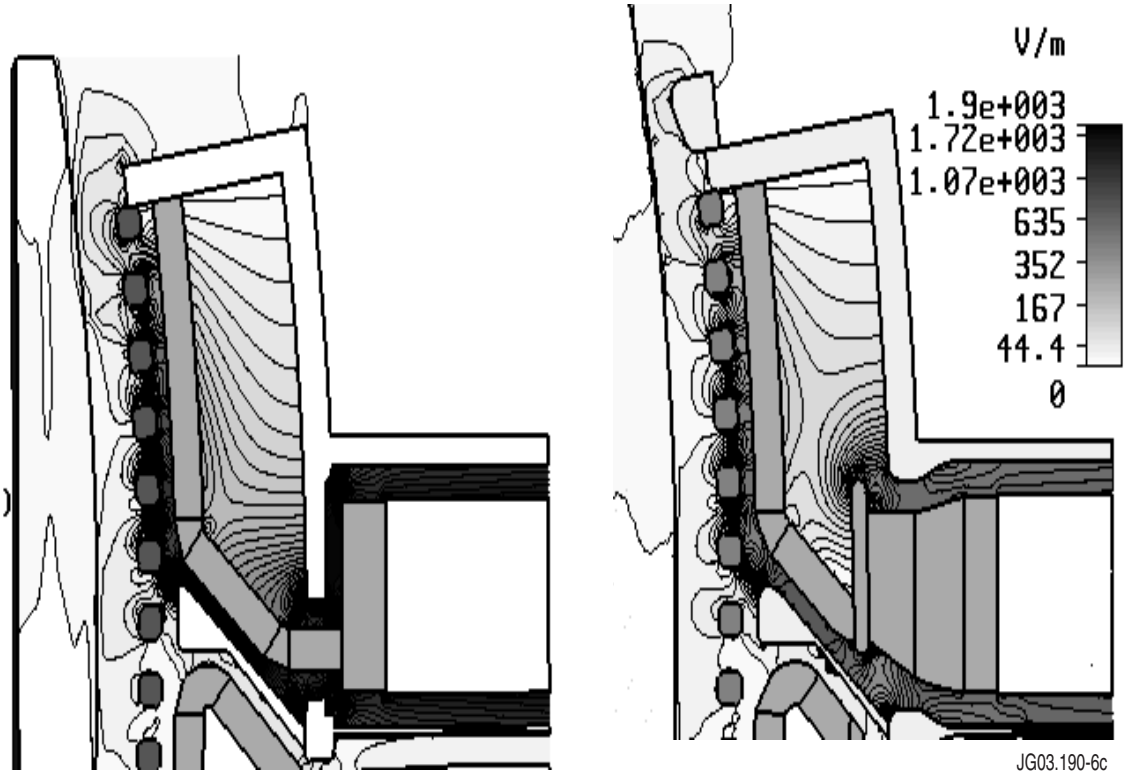


*Figure 2. Top strap with its feeder and capacitor sliding contact flange. Left: initial drawing; right: final layout. Shading according to electric field magnitude (Normalization to 1A short circuit current, scale from 0 to 1.9kV/m).*

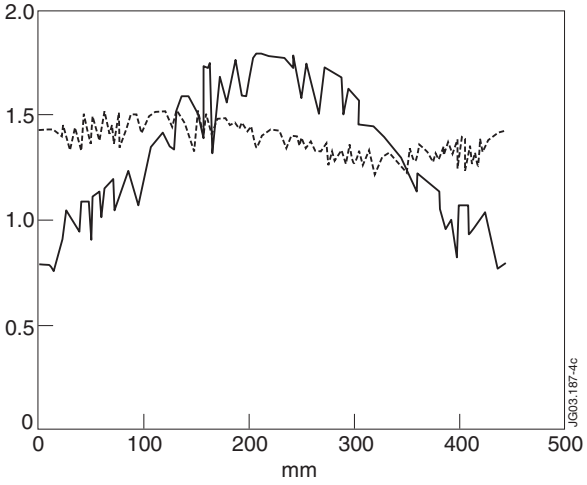


*Figure 3. Numerical current distribution along flange perimeter (for 1A at short-circuit). Plain line: initial drawing; discontinuous line: final layout (max. deviations from average: respectively 27% and 9%).*

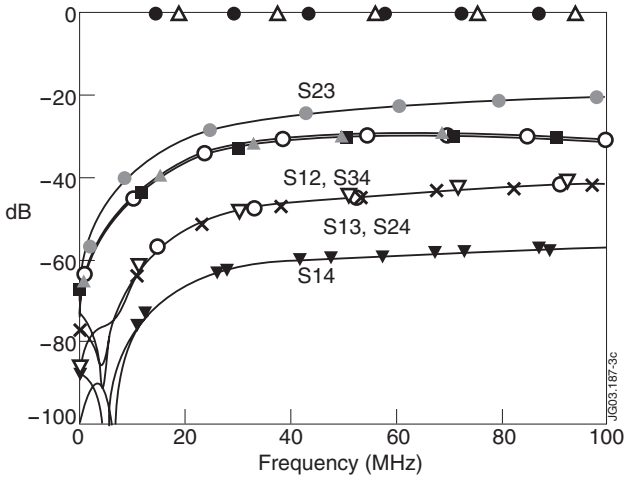


*Figure 4. Input scattering parameter amplitudes versus frequency in toroidal dipole phasing (ports are numbered from top to bottom).*

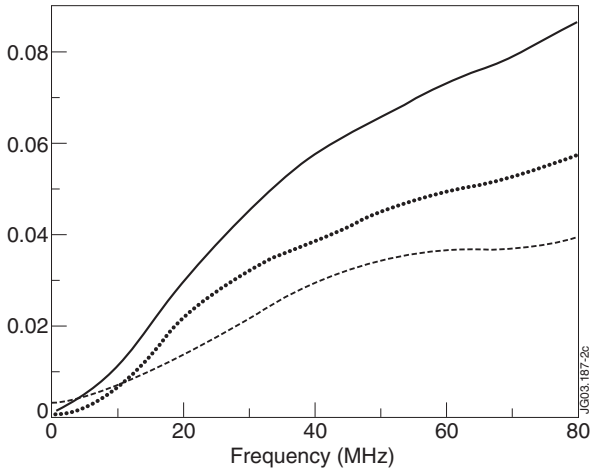


*Figure 5. Simulated poloidal cross-talk |S23| between inner straps. Plain, dotted, dashed lines: respectively, reference design; after extension of equatorial septum; and after closure of Faraday shield gap, predicting a factor-of-2 reduction.*

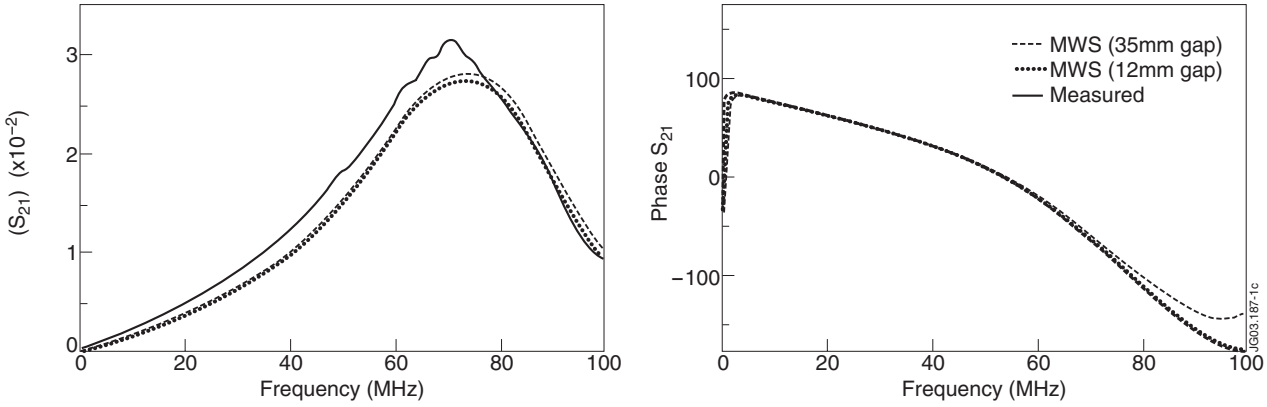


*Figure 6: Frequency response of scattering parameter S21 on 2-strap antenna prototype. Comparison between measurement and MWS model (the latter was run for 2 positions of the Farady shield). Left: amplitude; right: phase in degree.*